Nature Communications

https://doi.org/10.1038/s41467-026-69580-0

Article in Press

Portable hip exoskeleton improves walking economy for stroke survivors

Received: 28 May 2025

Accepted: 24 January 2026

Cite this article as: Pruyn, K., Murray, R., Gabert, L. *et al.* Portable hip exoskeleton improves walking economy for stroke survivors. *Nat Commun* (2026). https://doi.org/10.1038/s41467-026-69580-0

Kai Pruyn, Rosemarie Murray, Lukas Gabert, K. Bo Foreman & Tommaso Lenzi

Portable Hip Exoskeleton Improves Walking Economy for Stroke Survivors

Kai Pruyn[1,2], Rosemarie Murray[1], Lukas Gabert[1], Bo Foreman[1,3], and Tommaso Lenzi[1,2,4]*

1. Department of Mechanical Engineering at the University of Utah, Salt Lake City, UT, USA
2. The Rocky Mountain Center for Occupational and Environmental Health, Salt Lake City, UT, USA
3. Department of Kinesiology and Athletic Training at the University of Utah, Salt Lake City, UT, USA
4. Department of Biomedical Engineering at the University of Utah, Salt Lake City, UT, USA
***Corresponding author: t.lenzi@utah.edu**

Increased metabolic cost of walking after stroke limits mobility and quality of life for millions of individuals. Existing portable assistive devices, primarily targeting the ankle joint, have failed to alleviate this burden. Here, we tested a portable, lightweight hip exoskeleton providing bilateral assistance during walking for individuals with chronic post-stroke hemiparesis. The exoskeleton significantly reduced the net metabolic cost of walking by 18 ± 2% (mean ± standard error, p = 0.0002) in seven participants during treadmill walking—a reduction sufficient to potentially lessen fatigue and extend walking duration— compared to walking without the device. This improvement was associated with a 29 ± 6% reduction in positive biological hip work (p = 0.0052), indicating effective offloading of the hip joints. These results provide the first evidence that portable hip exoskeleton assistance can improve walking economy in stroke survivors, offering a promising therapeutic strategy to enhance real-world mobility and functional recovery in this large clinical population.

Millions of individuals experience reduced mobility and quality of life after a stroke[1,2]. Hemiparesis affects 80% of stroke survivors and is the leading cause of disability in the United States[3]. This condition involves impaired motor control[4], muscle weakness[5], and spasticity on one side of the body[6], which collectively contribute to challenges in community ambulation[7,8].

Independent walking is essential for enhancing community participation and quality of life after stroke [8,9]. Unfortunately, even after receiving the best rehabilitation and physical therapy, many stroke survivors face permanent impairments. Typically, individuals with hemiparesis have slow walking speeds[10], limited endurance[11], and high fall risk[12], diminishing their walking independence. These challenges primarily result from the inefficiency of hemiparetic gait patterns. The metabolic cost of walking in individuals with hemiparesis is 60% higher than in healthy populations[13], creating a significant physiological burden that directly limits functional endurance. This excessive effort often restricts individuals' ability to walk distances required for community engagement, contributes to debilitating fatigue, and ultimately diminishes independence and quality of life[2]. Therefore, reducing this metabolic burden is a critical clinical goal, and new devices and interventions are urgently needed to improve walking economy for those affected by hemiparesis.

Individuals with hemiparesis exhibit abnormal gait patterns due to the weakness of their affected side[10]. Ankle weakness typically leads to impaired push-off during late stance, decreasing propulsion[4,14]. Ankle weakness also contributes to a lack of dorsiflexion during swing (foot drop), reducing foot clearance and increasing fall risk[15]. Knee weakness leads to instability during early stance, forcing individuals with hemiparesis to hyperextend their knee for stability[4,16]. This hyperextension increases loading on the knee, which can increase pain and the risk of secondary conditions, such as osteoarthritis[17,18]. Furthermore, knee spasticity can lead to stiff knee gait, characterized by a lack of knee flexion during swing[14]. Finally, hip weakness impairs swing initiation, leading to shorter steps and decreased gait symmetry[19,20]. Compensatory movements, such as hip hiking and circumduction, are commonly used to compensate for foot drop and stiff knee gait[21]. Moreover, the unaffected side must compensate for the weakness and lack of coordination of the affected side, making hemiparetic gait highly asymmetric. These abnormal gait patterns result in a substantial increase in the metabolic cost of walking[22–24]. Thus, new devices and interventions that directly target leg weakness and abnormal gait could improve metabolic cost of walking in the hemiparetic population.

Powered exoskeletons are a potential solution to this problem[25]. Exoskeletons can supplement the affected joint's residual strength using power from motors and have been previously studied to assist hemiparetic gait[26–28]. However, achieving substantial metabolic cost reductions with portable devices in clinical populations such as stroke survivors remains a significant challenge[25].

Substantial research efforts have focused on using powered ankle exoskeletons or exosuits to improve paretic ankle propulsion[29–31]. One study demonstrated that improving propulsion decreased the metabolic cost of walking in individuals with hemiparesis[27]. However, this study used a tethered device to offset the mass of the actuators, battery, and control electronics, making the device unusable outside the lab. The additional mass of an exoskeleton increases metabolic cost proportionally to its distance from the user's center of mass, so carrying mass at the ankle is four times more costly than carrying mass at the trunk[32]. To partly

address this problem, portable versions of the ankle exosuit located the actuation, battery, and electronics in a hip pack, which minimizes the metabolic penalty of the additional mass[33]. This portable ankle exosuit demonstrated increased overground walking speed[27,34]. However, it did not decrease the metabolic cost of walking or transport[34–36]. As such, no portable ankle exoskeleton has successfully reduced the metabolic cost of walking for individuals with hemiparesis, most likely due to the added exoskeleton weight.

Powered hip exoskeletons can be very lightweight[37–40], minimizing the metabolic penalty of the additional mass. Furthermore, the mass of a hip exoskeleton creates less burden on the body because it is located closer to the body's center of mass, thereby minimizing the metabolic energy cost of carrying it[32]. The peak torque and power are lower at the hip joint than at the ankle joint[41], allowing hip exoskeletons to have smaller motors and batteries. In contrast to ankle exoskeletons, which can only inject energy during stance when the foot is in contact with the ground, hip exoskeletons can inject additional energy during swing. Pathological conditions that result in decreased ankle push-off demand greater positive hip flexion and extension power[42–44], which is metabolically more costly than positive ankle power[45]. Thus, powered hip exoskeletons are a promising solution to assist hemiparetic gait.

Although many studies have demonstrated the metabolic benefits of powered hip exoskeleton assistance in healthy individuals[39,40,46–56], only a handful of studies have explored hip exoskeletons to assist individuals with hemiparesis[57–60]. Unilateral hip exoskeleton assistance to the hemiparetic side has shown improved walking speed[57,58]. Moreover, bilateral assistance to both hips has shown greater improvements in walking speed than unilateral assistance to the affected hip joint only[58,59]. A case series with three individuals with hemiparesis subjects suggested that unilateral hip flexion assistance could improve the metabolic cost of walking[61]. However, a subsequent study with nine hemiparetic subjects showed no significant improvement in the metabolic cost of walking with bilateral hip assistance[60]. Unfortunately, these studies did not assess the impact of hip assistance on hemiparetic gait biomechanics. As a result, it remains unknown whether concurrent hip flexion and extension assistance provided by a powered hip exoskeleton can effectively compensate for impaired ankle propulsion and reduce metabolic cost.

Biomechanical analysis has shown that using a hip exoskeleton to assist with hip flexion and extension can help compensate for reduced ankle propulsion associated with a passive leg prosthesis[62] thereby decreasing the metabolic cost of walking in individuals with above-knee amputation[63]. Based on these findings, we hypothesize that a hip exoskeleton could offset the impaired ankle propulsion in individuals with hemiparesis by simultaneously assisting the affected and unaffected hip joints, leading to reduced metabolic cost and positive biological work of both hip joints. To test this hypothesis, we assessed the metabolic cost of treadmill walking at a constant self-selected speed, with and without a lightweight, portable, bilateral hip exoskeleton designed to supplement the user's hip flexion and extension, while measuring the positive biological work performed by both hip joints.

Results

We conducted experiments with individuals with hemiparesis after stroke (n=7) walking with and without a lightweight, portable, bilateral hip exoskeleton (Fig. 1a-b). The exoskeleton provided flexion assistance during late stance and swing and extension assistance during early-to-mid stance to the affected and unaffected hip joints (Supplementary Fig. 1). The assistance was manually tuned for each participant and each side independently, based on the participant's subjective feedback and the experimenter's judgment. The total weight of the exoskeleton was 2.63 kg. Participants walked on a fully instrumented, split-belt treadmill (Bertec) for six minutes at a time with and without the powered hip exoskeleton. The treadmill speed was based on the participants' overground walking speed, measured using the 10-meter walk test. Data were recorded during the last 2 minutes of each treadmill walking trial. Pairwise t-tests were performed to assess significant differences in our three primary outcome measures: metabolic cost of walking, total positive biological work, and positive biological hip work, with and without the exoskeleton. See Materials and Methods for more details.

Metabolic cost

The metabolic cost of walking was calculated for each participant as the total metabolic energy expenditure minus the metabolic consumption during relaxed standing[32,64]. The average net metabolic rate was 2.8 ± 0.1 W kg^{-1} (mean ± standard error of the mean) without the exoskeleton and decreased to 2.3 ± 0.1 W kg^{-1} with the exoskeleton assistance (Fig. 1c). Thus, assistance from the powered exoskeleton reduced the metabolic cost of walking by 18 ± 2% on average across the seven participants (two-tailed paired *t*-test, p = 0.0002). All participants showed a reduction in the metabolic cost with the exoskeleton compared to walking without the exoskeleton (Fig. 1c).

To account for the metabolic cost of wearing the exoskeleton, we calculated the metabolic penalty of adding exoskeleton mass to the thigh and pelvis[64,65]. The exoskeleton mass added to each thigh was 0.67 kg, resulting in a metabolic penalty of 7.44 W (5.55 W kg^{-1} x 0.67 kg/side x 2 sides). The exoskeleton mass added to the pelvis was 1.29 kg, resulting in a metabolic penalty of 4.23 W (3.33 W kg^{-1} x 1.29 kg). Thus, the total metabolic penalty of wearing our portable hip exoskeleton was 11.76 W, which, normalized by the body weight of each participant and averaged, is equivalent to 0.148 W kg^{-1}.

Accounting for the estimated metabolic penalty of the exoskeleton mass, the theoretical net metabolic savings compared to wearing the unpowered exoskeleton would be 0.653 W kg^{-1}, compared to the measured 0.505 W kg^{-1} without the exoskeleton. Given that the average positive mechanical power for both exoskeleton sides combined was 0.317 W kg^{-1}, the average ratio between the weight-adjusted metabolic saving and the average positive bilateral exoskeleton power across subjects was 2.06 (Supplementary Fig. 2). Thus, if we account for the metabolic penalty of the exoskeleton mass, the average modified exoskeleton performance index[65,66] was 0.515, which is about half the theoretical maximum of 1 (Supplementary Table 1).

To assess the metabolic cost of walking in a speed-normalized form, we calculated the cost of transport[67]. The average cost of transport with the exoskeleton was 3.6 ± 0.4 J m^{-1} kg^{-1}, down from 4.4 ± 0.5 J m^{-1} kg^{-1} without the exoskeleton. As expected from the metabolic rate analysis, all participants decreased their cost of transport with the exoskeleton. However, the reduction in the cost of transport was inversely proportional to the walking speed (Supplementary Fig. 3).

Positive joint work

As is commonly done in the field[46,68], we analyzed positive work as it has been shown to have a substantially higher metabolic cost than negative or total work[69]. Positive biological work (Fig. 2a-b) was calculated by integrating positive biological power. Biological hip joint power (Fig. 2c) with the exoskeleton is the total hip joint power calculated through inverse dynamics minus the exoskeleton power.

The total positive work done by the hip exoskeleton (affected and unaffected sides) per stride was 0.12 ± 0.01 J kg^{-1}. This exoskeleton assistance significantly reduced the total positive biological work by 14% ± 4% on average across the seven participants (two-tailed paired t-test, P = 0.0167). Specifically, the total positive biological work done by the affected and unaffected hip, knee, and ankle joints per stride decreased from 0.76 ± 0.07 J kg^{-1} without the exoskeleton to 0.66 ± 0.07 J kg^{-1} with the exoskeleton (Fig. 2a).

Exoskeleton assistance significantly reduced the positive biological hip work by 29% ± 6% on average across the seven participants (two-tailed paired t-test, P = 0.0052). Specifically, the positive biological hip work per stride decreased from 0.33 ± 0.05 J kg^{-1} without the exoskeleton to 0.23 ± 0.05 J kg^{-1} with the exoskeleton. In contrast, no significant differences in positive biological work were observed for the knee or ankle joints (Fig. 2a).

Without the exoskeleton, the total positive work per stride was 0.26 ± 0.03 J kg^{-1} on the affected side and 0.51 ± 0.05 J kg^{-1} on the unaffected side. With the exoskeleton, the total positive work increased by 0.02 ± 0.02 J kg^{-1} (8% ± 7%) on the affected side and was virtually unchanged on the unaffected side (-1% ± 5%).

On the affected side, the exoskeleton provided 21% ± 3% of the total positive work, and the biological hip joint contribution to total positive work decreased from 48% ± 6% to 35% ± 6% (Fig. 2b). On the unaffected side, the exoskeleton contributed 14% ± 1% of the total positive work, and the contribution of the unaffected hip joint decreased from 40% ± 4% to 25% ± 2% with the exoskeleton.

Hip work during stance

The exoskeleton assistance noticeably affected the biological hip joint power during different phases of the gait cycle (Fig. 2c). We assessed the effects of exoskeleton assistance on positive biological hip work within different gait phases:

initial double support, single support, terminal double support, and swing (Fig. 3). Initial double support lasts from the ipsilateral heel strike to the contralateral toe-off, then single support occurs during the contralateral swing phase, and finally, terminal double support occurs from the contralateral heel strike until the ipsilateral toe-off.

When the unaffected side is in initial double support, the affected side is in terminal double support (Fig. 3). During this critical step-to-step transition, the exoskeleton provides extension assistance to the unaffected side and flexion assistance to the affected side, decreasing the positive biological hip work by 0.026 ± 0.008 J kg^{-1} (60% ± 18%) and 0.022 ± 0.013 J kg^{-1} (49% ± 26%), respectively, per stride. During the next phase of gait, when the unaffected side was in single support and the affected side was in swing, the positive biological hip work also decreased by 0.035 ± 0.013 J kg^{-1} (64% ± 19%) and 0.014 ± 0.014 J kg^{-1} (55% ± 27%) on the unaffected and affected side, respectively. During the following step-to-step transition (unaffected side trailing), the positive biological hip work decreased slightly by 0.005 ± 0.009 J kg^{-1} (83% ± 25%) on the unaffected side but increased by 0.014 ± 0.009 J kg^{-1} (118% ± 22%) on the affected side. In the final phase, when the unaffected side is in swing and the affected side is in single support, the positive biological hip work decreased by 0.017 ± 0.004 J kg^{-1} (71% ± 17%) on the unaffected side and increased slightly by 0.004 ± 0.003 J kg^{-1} (168% ± 22%) on the affected side.

Foot clearance

Minimum foot clearance trajectories were calculated by taking the minimum trajectory of the toe and heel during swing (Supplementary Fig. 4). Hip exoskeleton assistance increased foot clearance on both the affected and unaffected sides. On the affected side, peak foot clearance increased by 4 ± 2 mm (10% ± 6%) with the exoskeleton. On the unaffected side, peak foot clearance increased by 3 ± 1 mm (7% ± 3%) with the exoskeleton.

Kinematics

Kinematic trajectories during walking with and without the exoskeleton are presented in Supplementary Fig. 5. Hip exoskeleton assistance slightly increased the affected hip joint's average range of motion (Supplementary Fig. 6), primarily by increasing peak hip flexion by 2° ± 1° (8% ± 3%). The unaffected hip joint's average range of motion decreased by 2° ± 1° (8% ± 2%), decreasing in both peak flexion and extension. Exoskeleton extension assistance slightly increased the average peak knee extension angle by 2° ± 1° (31% ± 18%) on both sides. Finally, with the exoskeleton, the affected ankle joint was slightly more plantarflexed throughout the gait cycle, while the unaffected ankle joint was slightly more dorsiflexed throughout the gait cycle. These differences were generally less than 2° and resulted in a slightly decreased range of motion at the affected ankle joint (Supplementary Fig. 6). Statistical Parametric Map (SPM) analysis demonstrated that there were no statistically significant differences (two-tailed paired t-test, $\alpha = 0.05$) in the kinematic trajectories of each joint during walking with the exoskeleton compared to without the exoskeleton (Supplementary Fig. 7). Thus, hip exoskeleton assistance resulted in only minor, non-clinically significant and non-statistically significant kinematic changes.

Symmetry was evaluated by calculating a symmetry index (SI) where 0% indicates perfect symmetry[36]. Hip exoskeleton assistance improved symmetry in the hip joint range of motion (-30% ± 10% without the exoskeleton vs. -18% ± 9% with the exoskeleton) but had only minor effects on the knee and ankle range of motion symmetry (Supplementary Fig. 8). Exoskeleton assistance slightly improved symmetry in stance time (13% ± 3% asymmetry without the exoskeleton vs. 12% ± 4% asymmetry with the exoskeleton), but increased asymmetry in step length (-8.2% ± 6% without the exoskeleton vs. -14% ± 5% with the exoskeleton) (Supplementary Fig. 9). Generally, during walking with and without the exoskeleton, participants spent longer in stance on their unaffected side and took longer steps onto their affected side.

To evaluate gait stability, we compared the extrapolated center of mass and step width during walking with and without the exoskeleton (Supplementary Fig. 10). The minimum mediolateral distance from the extrapolated center of mass to the average center of pressure of the affected and unaffected sides was relatively unchanged, decreasing by 0.2 ± 0.3 cm (5% ± 8%) on the affected side and by 0.06 ± 0.34 cm (4% ± 11%) on the unaffected side with the exoskeleton. Furthermore, the step width was 20 ± 2 cm during walking with and without the exoskeleton.

Kinetics

Kinetic trajectories, including the biological hip, knee, and ankle joint moment and vertical ground reaction force (GRF) trajectories are presented in Supplementary Fig. 11. On the affected side, exoskeleton assistance increased the average peak biological hip flexion and extension moments on the affected side by 0.07 ± 0.09 Nm kg^{-1} (3% ± 17%) and 0.07 ± 0.04 Nm kg^{-1} (38% ± 27%), respectively. On the unaffected side, exoskeleton assistance increased the peak biological hip flexion moment by 0.13 ± 0.09 Nm kg^{-1} (27% ± 19%) and decreased the peak biological hip extension moment by 0.10 ± 0.04 Nm kg^{-1} (20% ± 7%). Similarly, on the affected side, hip exoskeleton assistance increased the peak knee flexion moment by 0.10 ± 0.03 Nm kg^{-1} (21% ± 9%) and decreased the peak knee extension moment by 0.09 ± 0.04 Nm kg^{-1} (48% ± 23%). In contrast, on the unaffected side, exoskeleton assistance decreased the peak knee flexion moment by 0.0002 ± 0.0300 Nm kg^{-1} (0.6% ± 8.4%) and increased the peak knee extension moment by 0.10 ± 0.05 Nm kg^{-1} (27% ± 17%). Finally, the ankle moments were unchanged on both the affected and unaffected sides during walking with exoskeleton assistance compared to walking without the exoskeleton. The greater peak joint moments with hip exoskeleton assistance are likely related to the greater observed vertical ground reaction force. The peak vertical GRF increased by 0.04 ± 0.006 N kg^{-1} (4.4% ± 0.6%) on both the affected and unaffected sides (Supplementary Fig. 12).

Exoskeleton assistance

Many participants preferred similar exoskeleton tuning on each side, resulting in similar generated torque profiles on each side. Notably, participant 6 received greater peak flexion torque on their affected side compared to their unaffected side. Generally, the peak flexion torque provided by the exoskeleton was greater than the peak extension torque, with greater extension torque supplied to the unaffected side (Supplementary Fig. 1). Each peak of exoskeleton torque resulted in a positive exoskeleton power peak, with flexion torque resulting in a greater peak power than extension torque. The peak power generated on the unaffected side was greater than that generated on the affected side for both flexion and extension assistance. Specifically, the peak power generated on the unaffected side (0.17 ± 0.02 W kg^{-1} flexion, 0.09 ± 0.01 W kg^{-1} extension) was greater than that generated on the affected side (0.13 ± 0.02 W kg^{-1} flexion, 0.08 ± 0.01 W kg^{-1} extension) for both flexion and extension assistance.

Handrail forces

For safety, all participants were instructed to rest their unaffected hand on a force-instrumented handrail mounted on the side of the treadmill, using only the minimum support needed. The average total handrail force was generally low, ranging from 1% to 5% of the participant's body weight (Table 1), and there was no statistically significant difference between the average total handrail force applied with and without the exoskeleton. Moreover, average handrail forces in the lateral, frontal, and vertical axes were very similar with and without the exoskeleton (Supplementary Fig. 13). However, the peak lateral handrail force occurred slightly earlier in the gait cycle when using the exoskeleton. The average handrail forces per stride in each axis remained the same with and without the exoskeleton. Some participants showed small differences in peak forces in each direction of their handrail forces, which can be seen when examining each plane of motion separately (Supplementary Fig. 14). The largest differences in handrail use were observed for participant 2, whose peak vector total handrail force increased by 2.2%, and participant 6, whose peak vector total handrail force decreased by 2.5%, with the exoskeleton per stride. On average, three participants used slightly more force with the exoskeleton (S2, S3, S4), while four participants used slightly less force (S1, S5, S6, S7).

Discussion

Individuals with hemiparesis have a significantly higher metabolic cost of walking than healthy individuals[2,22,24], limiting physical activity[8], community participation, and reducing overall health and quality of life[1,3,9]. Portable powered exoskeletons have successfully improved the metabolic cost of walking in young, healthy individuals[39,40,46–51,53–56], but have not yet done so in individuals with hemiparesis[25,60]. Here we show that assistance from a lightweight, portable, bilateral hip exoskeleton decreased the metabolic cost of walking in individuals with hemiparesis (n=7) by 18%, equivalent to removing a 13.5-kg backpack from a healthy individual[32] (Fig. 1c). The observed metabolic cost reduction is substantial and has the potential to improve mobility and quality of life after stroke.

The reduction in the metabolic cost of walking obtained in this study using a portable hip exoskeleton (18%) is substantially greater than the metabolic reduction previously achieved using an ankle exosuit tethered to a benchtop actuator (10%)[27]. A case series with three individuals with hemiparesis suggested potential for unilateral hip flexion assistance to reduce the metabolic cost of walking[61]. Still, they found a much lower reduction compared to this study (8.6%), and no follow-up studies confirmed its statistical significance. Thus, our analysis suggests that bilateral, bidirectional hip assistance may be more effective than unilateral, unidirectional hip assistance and ankle assistance in improving the metabolic cost of walking with a portable exoskeleton or exosuit.

The metabolic penalty of wearing our portable hip exoskeleton was estimated at 11.76 W, similar to the average metabolic penalty of other advanced hip exoskeletons (6.93 – 17.7 W, Supplementary Table 1). When accounting for this metabolic penalty, the performance index of our exoskeleton was 0.515, well below the theoretical maximum of 1, which would indicate perfect energy transfer between the exoskeleton and the user. The apparent efficiency of our device is notably lower than that of portable power hip exoskeletons measured in previous studies with healthy subjects (0.515 versus 0.74-0.92, Supplementary Table 1). This difference may indicate that greater positive mechanical energy is necessary to achieve the same metabolic benefits in individuals with hemiparesis compared to healthy subjects.

Notably, the performance index calculation relies on two crucial assumptions that have not been verified[65,66]. The first assumption is that the metabolic penalty of adding mass to different leg segments in individuals with hemiparesis is the same as in healthy individuals[65] and does not change with walking speed. The second assumption is that muscles generate positive mechanical work with a muscular efficiency that asymptotically approaches 0.25[66,69] for both healthy individuals and those with hemiparesis, regardless of the walking speed. Future studies should examine the validity of these assumptions by comparing the exoskeleton performance index in healthy individuals and individuals with hemiparesis using the same device and assistive strategy.

All participants reduced their metabolic cost of walking with the exoskeleton. However, the self-selected walking speeds varied widely among participants (0.37 m s^{-1} – 1.00 m s^{-1}). To account for these differences in speed, we analyzed the cost of transport, which is a speed-normalized representation of metabolic walking effort[67]. As expected, the cost of transport decreased with walking speed both with and without the exoskeleton (Supplementary Fig. 3). The slowest participants exhibited the greatest reductions in the cost of transport with exoskeleton assistance, even though the metabolic rate reductions were approximately the same (Fig. 1). On average, the cost of transport decreased by 0.8 J m^{-1} kg^{-1} with the exoskeleton, which is equivalent to increasing walking speed by 0.16 m s^{-1}, assuming a linear relationship between cost of transport and walking speed within the observed range of speeds. This result suggests that the proposed assistive exoskeleton could enable hemiparetic subjects to increase their walking speed, in agreement with previous studies[57–59].

Individuals with hemiparesis typically compensate for impaired ankle propulsion by using their hip joints to provide extra energy during gait[20]. Our results show that exoskeleton assistance concurrently provided to the affected and unaffected hip joints assists with this compensation strategy by significantly reducing the positive biological work done by the hip joints (-29%). The reduction of positive hip work resulted in a significant overall reduction of positive biological work (-14%), even though the positive biological work at the knee and ankle did not change (Fig. 2a). This finding provides important mechanistic insight into how hip assistance influences walking energetics post-stroke, demonstrating effective offloading of the user's joints and suggesting that the metabolic benefit stems directly from this reduction in biological effort, rather than complex compensations elsewhere. Understanding these biomechanical underpinnings is crucial for optimizing future device designs and control strategies.

As expected, without the exoskeleton, the unaffected side provided more positive work per stride than the affected side (0.50 J kg^{-1} unaffected side vs. 0.26 J kg^{-1} affected side). With the exoskeleton, the total positive work per stride on the affected side, including the positive exoskeleton work, increased by 11% (Fig. 2b). However, it remained lower than the unaffected side positive work (0.51 J kg^{-1} unaffected side vs. 0.28 J kg^{-1} affected side). The total positive work on the unaffected side remained unchanged with the exoskeleton. On both the affected and unaffected sides, the exoskeleton assistance contributed significantly to the positive work done by the hips. Thus, exoskeleton assistance improved symmetry in the total work done by the affected and unaffected sides while generally decreasing the contribution of the biological hips to the total positive work.

The positive biological hip work on the unaffected side decreased for all gait phases with the exoskeleton (Fig. 3). In contrast, the positive biological hip work on the affected side

decreased during terminal double support and the subsequent swing, but increased during initial double support and the following single support. Although greater positive biological work is generally detrimental to metabolic cost[69], the observed increase in positive biological work during initial double support also indicates that the affected side more closely matches the unaffected side. Therefore, exoskeleton assistance might help the affected hip generate more typical positive biological work during initial double support and single support.

The exoskeleton assistance was manually tuned for each participant. The experimenter adjusted the assistance parameters to maximize positive exoskeleton power generation based on the online estimates shown in the exoskeleton graphical user interface while ensuring patient safety and comfort through visual inspection and subjective feedback from the participants. The exoskeleton provided predominantly positive power on both sides, although peak power was greater on the participants' unaffected side than on their affected side for both flexion and extension, likely due to the smaller range of motion of the affected side. In agreement with previous studies showing that positive exoskeleton power is critical for reducing the metabolic cost of walking[47,70], the participant with the exoskeleton assistance profile with the most negative power also had the smallest metabolic cost reduction (S3, 8%). Although we did not observe a strong correlation between positive exoskeleton power and metabolic cost reduction, this study confirms that positive power is key to reducing metabolic rate.

Generally, participants preferred greater flexion torque than extension torque and greater torque on their unaffected side than their affected side (Supplementary Fig. 1). Despite these general trends, the exoskeleton torque profiles vary widely between subjects. Participant 3, who showed the smallest metabolic reduction, had the latest timing for peak flexion and extension assistance during the gait cycle, which may have contributed to the generation of large amounts of negative power from the assistance profiles. Participants 2 and 3 received the lowest peak flexion and extension torques and had the smallest reductions in metabolic cost, which could indicate a relationship between peak assistive torque and metabolic reduction. On the other hand, participant 6 received the greatest peak flexion torques but did not achieve the largest reduction in metabolic cost, indicating that a more nuanced interpretation is needed.

Hip exoskeleton assistance had a small effect on the hip joint range of motion for both sides (Supplementary Fig. 5-6). Specifically, the exoskeleton assistance increased the affected hip joint's range of motion by 2° and decreased the unaffected hip joint's range of motion by 2°, improving symmetry in hip joint range of motion by 12% (Supplementary Fig. 8). The observed kinematic changes are small and below the thresholds for clinical and statistical significance (Supplementary Fig. 7). Furthermore, we did not observe any meaningful changes in the extrapolated center of mass and step width, indicating that hip exoskeleton assistance did not adversely affect stability (Supplementary Fig. 10). Hip exoskeleton assistance slightly improved symmetry in stance time but decreased symmetry in step length (Supplementary Fig. 6). The observed increase in step length asymmetry indicates that the participants take longer steps onto their affected side with the exoskeleton assistance. This result is likely due to the assisted hip flexion during swing. Overall, we did not observe any consistent trends in spatiotemporal variables across participants during walking with the exoskeleton compared to walking without the exoskeleton. Although passive[71] and powered[26] ankle-foot orthoses/exosuits have shown consistent improvements in symmetry for stance time and step length, previous powered hip exoskeleton studies have not[58–60]. Our results seem to confirm that portable powered hip exoskeletons do not consistently increase symmetry. This result may be due to the assistive controller being primarily tuned to provide positive power as needed to reduce metabolic rate.

Hip exoskeleton assistance increased the affected side peak foot clearance by approximately 4 mm (Supplementary Fig. 4). This improvement is equivalent to that observed from ankle-foot orthosis use[72] and assistance from a powered ankle exoskeleton in individuals with hemiparesis[35]. However, another powered ankle exoskeleton study achieved a much greater increase (approximately 2 cm) in individuals with hemiparesis[26]. Furthermore, a case study with another ankle exoskeleton demonstrated further increases in clearance, ranging from 3.6 cm to 5.4 cm, depending on walking speed, in one individual with hemiparesis[73]. Although the increase in foot clearance observed in this study is relatively small, it may reduce the risk of trips and falls in individuals with hemiparesis[15].

Although this study includes only a small sample size (n=7), the sample was diverse. The two female participants (S1 and S2) had an average metabolic cost reduction similar to that of the male participants (18% women vs 18% men). Two participants (S2, S6) used ankle-foot orthoses (AFO). The average metabolic cost reduction for these two participants was slightly less than for the others (17% vs 19%). This result suggests that individuals with ankle-foot orthoses may experience slightly less metabolic benefit from hip exoskeleton assistance, which could be due to the AFOs restricting ankle push-off and limiting gait adaptability[74,75]. We did not observe any other trends in the age, chronicity, weight, or other biological factors of the participants presented in Table 1. Our results indicate that hip exoskeletons can assist a wide range of individuals with hemiparesis based on level of impairment, size, sex, and use of other assistive devices. Further studies with a larger sample size are needed to assess important clinical and biological factors that may impact the efficacy of hip exoskeleton assistance.

This study focuses only on the immediate effects of exoskeleton assistance on walking performance. However, long-term benefits can potentially result from these immediate improvements. As pointed out in a previous exosuit study[27], immediate metabolic improvements may enable individuals to practice walking longer and at a higher intensity, which may promote neurorehabilitation[76–78].

Moreover, the observed improved walking performance may reduce barriers to community engagement[11,79,80], further promoting key plasticity mechanisms such as salience, intensity, and repetition during gait training[77,81,82].

Limitations

This study highlights the potential of powered exoskeletons to establish a new standard of care for individuals with hemiparesis after stroke. Although we received positive feedback from the study participants, we did not perform an official qualitative assessment, which is essential for acceptability in the real world. Future studies should investigate whether the results presented here can be extended to overground walking, including inclines and variable terrain, which are common during daily ambulation. We expect device and control optimization to be critical for the clinical success of the proposed intervention.

The manual tuning of the exoskeleton assistance was another limitation of our study. Control algorithms that automatically optimize powered exoskeleton assistance could also lead to further improvements. Human-in-the-loop optimization could be used in the future to optimize the exoskeleton assistance and minimize the metabolic cost of walking[83]. Tuning methods based on musculoskeletal modeling could also optimize exoskeleton assistance while reducing tuning time[84]. Finally, assistance tuning methods based on artificial intelligence and machine learning could be used to adapt the exoskeleton assistance for different inclines[46]. Future work in developing control methods based on human-in-the-loop optimization, biomechanical modeling, and artificial intelligence or machine learning may further improve the metabolic cost of walking, gait symmetry, kinematics, and other outcomes.

The exoskeleton assistive torque profiles indicate that a relatively small peak torque, between 5 Nm and 12 Nm, is sufficient for significant metabolic improvements. This torque level is much lower than the peak torque capabilities of the hip exoskeleton used in this study (45 Nm[37]). This result suggests that future powered hip exoskeletons should be designed to achieve a lower peak torque than the current design. This change in actuation requirements may result in lighter devices, potentially leading to greater improvements in metabolic cost.

Previous studies in healthy young individuals suggest that powered exoskeletons have the potential to reduce joint loading[85], which has been previously linked to the increased incidence of osteoarthritis. In this study, we could not perform this analysis due to the lack of electromyography, which is needed to validate the biomechanical simulations estimating joint loading. Future studies should evaluate the effects of exoskeleton assistance on hip, knee, and ankle joint loading in individuals with hemiparesis. Finally, future research should examine the long-term effects of hip exoskeleton assistance, including pain and risk of secondary conditions.

Methods

Participants

We recruited seven individuals with hemiparesis from local clinics to participate in this study. Participant inclusion criteria included the following: age between 18 and 85 years, at least 6 months post-stroke, hemiparesis due to stroke, and the ability to walk on a treadmill for six minutes. Participants were excluded from the study if they weighed more than 250 lbs or had a cognitive deficiency that precluded the ability to give informed consent, were pregnant, or had a co-morbidity that interfered with the study. Following statistical power analysis, we enrolled seven participants (Table 1).

Ethics

The Institutional Review Board at the University of Utah approved the study protocol (IRB 00120712). Participants provided written informed consent to participate in the study. Participants also provided written consent for the publication of pictures and videos of the experiments.

Exoskeleton training and assistance tuning

Participants underwent extensive training with the hip exoskeleton before the metabolic cost evaluation and motion capture experiment (Fig. 4). Training with the exoskeleton allows users to adapt and maximize the benefits of the assistance[86]. It can take hours of training for individuals with mobility challenges to experience maximum benefits from exoskeleton assistance[87]. Due to the neurological impact of a stroke, motor adaptation is critical for individuals with hemiparesis to optimize the benefits of exoskeleton assistance[88]. To allow sufficient training, participants came in for exoskeleton training sessions and completed at least 30 minutes of continuous walking with the exoskeleton before data collection (Fig. 4b).

The first training session included fitting the exoskeleton for each participant. The experimenter helped the participants don the powered hip exoskeleton and adjusted the straps to ensure a proper fit while alleviating potential discomfort. After fitting the device, the participants walked on a treadmill, and the experimenter manually tuned the assistive controller by adjusting the timing and peak of the flexion and extension torques. To maximize assistance, the experimenter watched a real-time plot of the estimated joint power and adjusted the controller parameters while the participant walked with the exoskeleton. This tuning procedure was done independently for the affected and unaffected sides. Exoskeleton assistance parameters were tuned based on the experimenter's training and experience via visual inspection of gait during the walking sessions[89]. The experimenters also watched a live estimate of exoskeleton power based on the exoskeleton torque and velocity, and adjusted timing and peak torque parameters to maximize positive power generation, which is critical for reducing the metabolic cost of healthy subjects[47,70]. After each adjustment, the participant was asked if the assistance felt better or worse. If it felt better, the experimenter would continue adjusting that parameter in that direction until it felt worse. If the change felt worse, the parameter was reverted to its previous value, and a different change was made. Comfort was assessed by asking the participants for their subjective feedback and visually inspecting the exoskeleton interfaces for excessive bending or movements. Participants walked for approximately half an hour, less than 10 minutes at a time, with rest between walking trials.

Each additional training session was completed approximately one week apart. These sessions included at least half an hour of total walking with the device, where participants walked for less than 10 minutes at a time with rest in between walking trials. The experimenter continued tuning the exoskeleton assistance as necessary. The experimenter determined when to advance the participant in the protocol based on their experience and the participant's feedback on their comfort and confidence with the device. All participants completed at least one training session before completing data collection.

The amount of exoskeleton training was not standardized across participants in this study to accommodate differences in walking ability between participants. Some participants exhibited less consistent walking patterns, which made exoskeleton tuning less consistent and necessitated more tuning and training. Furthermore, some participants needed more rest and walked less each training day, so they had more training days than participants who could walk longer in one session. On average, participants completed 2±1 additional training sessions (not including the fit/tune session) before data collection. Participants generally completed a session once a week, completing training over 4±1 weeks on average. The experimenter started with the converged parameters from the prior training session and tuned as necessary from there. Parameters were retuned in each training session based on any changes in user preference or comfort, and any gait changes observed by the experimenter. The exoskeleton parameters were kept the same as the final tuned parameters from the final training session during the metabolic cost evaluation and motion capture experiments.

Metabolic cost evaluation

Approximately one week after the participants completed the exoskeleton training, we evaluated their metabolic cost of walking with and without the powered exoskeleton (Fig. 4c). Participants donned a heart rate monitor (Polar). They performed a 10-meter walk test twice to determine their self-selected walking speed. Participants then donned a portable indirect calorimetry measurement system (K5, COSMED) and performed the final stage of the metabolic system calibration[90].

At the beginning of the experiment, participants stood still for 2 minutes while their baseline standing metabolic rate was collected. Next, the participants walked on a fully instrumented, split-belt treadmill (Bertec) at their self-selected walking speed for 6 minutes to determine the metabolic cost of walking without the exoskeleton. Data were collected during the last 2 minutes of the walking trial.

Participants rested seated until their heart rate reached their baseline resting rate. Then, the participants donned the

powered hip exoskeleton. After ensuring proper fit, the participants walked with the exoskeleton on the treadmill at the same walking speed as without the exoskeleton. To allow sufficient time for acclimatization[88], participants performed three treadmill walking trials while wearing the exoskeleton, as in other metabolic studies[28,63]. Each walking trial consisted of a slow increase in assistance for 1 minute, followed by 6 minutes of walking. Thus, each participant walked with the exoskeleton assistance for 21 minutes. Data were collected during the last 2 minutes of the third walking test. Before each test, the participants rested seated for at least 5 minutes, or until their heart rate reached their baseline resting rate. Upon completion of the three exoskeleton walking trials, the participants rested. After the final rest, we measured their standing metabolic expenditure to check for fatigue.

For safety, all participants were instructed to rest their unaffected hand on a side-mounted handrail during all treadmill walking tests. We instructed participants to use the smallest amount of handrail support needed, and the level of support was different for each participant. The average vector total handrail force per stride ranged between 1% and 5% of each participant's body weight (Table 1). Participants were generally consistent with the level of support they used with and without the exoskeleton, and only two participants showed meaningful differences between exoskeleton conditions. Participant 2 increased their peak vector total handrail force by 2.2% with the exoskeleton, while participant 6 decreased their peak vector total handrail force by 2.5% with the exoskeleton. Participants wore a harness, but no body weight was supported.

The appearance of the conditions was not randomized, and participants always walked without the exoskeleton first. Randomizing the appearance of the exoskeleton and no exoskeleton conditions could have disrupted the adaptation period and introduced aftereffects[59,91]. Moreover, it would have been impractical because it would have required participants to repeatedly don and doff the exoskeleton, requiring additional time to ensure the proper fit of the exoskeleton and recalibrate the motion capture system, contributing to fatigue. The lack of randomization may have introduced bias. For example, if the participants became fatigued during the session, we would expect that their metabolic cost would have increased between the first and last 6-minute walking trials. To ensure fatigue was not a problem, we compared the initial standing baseline taken before the walking tests to the standing baseline after the tests with the exoskeleton. This also allowed us to assess potential drifts in the respiratory measurements. There was no statistical difference between the standing metabolic expenditure measured at the beginning and end of the protocol. Thus, respiratory measurements showed no significant drifts, and participants did not experience fatigue.

Motion capture experiment

Compared to our previous metabolic study with individuals who have above-knee amputations[63], we added an experimental session to perform a comprehensive biomechanical analysis using full-body motion capture with an instrumented treadmill and instrumented handrails. This additional analysis provided a mechanistic explanation for the observed metabolic reduction, which is essential to assess the benefits of the proposed assistive approach.

Approximately one week after the metabolic cost evaluation, the final testing session was performed in a motion capture lab using a 12-camera Vicon system (Vicon Motion Systems, Ltd., Oxford, U.K.) and a fully instrumented split-belt treadmill (Bertec, Ohio, USA) (Fig. 4d). Participants wore tight-fitting clothing with reflective markers placed on anatomical bony landmarks. Markers were placed following a modified Plug-in-Gait model with redundant markers placed on the hip, thighs, shins, and feet for more reliable tracking[92].

Each participant completed a static calibration trial, a functional joint center calibration trial, and a functional dynamic capture. These calibration routines were repeated twice, once without the exoskeleton and once with the exoskeleton. The static calibration created a subject-specific motion capture model. The functional joint center calibration located the centers of rotation for the hip and knee joint axes using the Symmetric Center of Rotation Estimation (SCoRE)[93] and Symmetrical Axis of Rotation Analysis (SARA)[94]. The functional dynamic capture improved the ability of the software to build and label the model for each additional capture.

Upon completion of the calibration trials, the participants repeated the series of 6-minute walking trials completed during the metabolic cost evaluation at the same speed and with the same exoskeleton tuning. Data were recorded during the last 2 minutes of the test without the exoskeleton and the third test with the exoskeleton. Marker trajectories were sampled at 200 Hz, and ground reaction forces were sampled at 1000 Hz. All data were synchronized using a lock sync box (Vicon Motion Systems, Ltd., Oxford, U.K.).

We conducted the metabolic cost evaluation and motion capture sessions on separate days to minimize the burden on participants and the potential for fatigue. To reduce the impact of day-to-day variability, we implemented exoskeleton training sessions before data collection and used the same treadmill walking speed and exoskeleton tuning during both experiments. A multi-day protocol also reduced the impact of data collection failures due to problems with the exoskeleton, metabolic, or motion capture equipment.

Powered hip exoskeleton

The powered hip exoskeleton used in this study was previously presented and validated in healthy individuals[37], individuals with above-knee amputation[63], and one individual with hemiparesis[57]. The exoskeleton provides bilateral flexion and extension torque to the user's hip joints while allowing for passive abduction and adduction. All interfaces, actuation, electronics, and the battery are integrated into the exoskeleton, which is worn on the user's pelvis and thighs. The total weight of the exoskeleton was up to 2.63 kg.

Compared to our previous metabolic study with individuals who have above-knee amputations[63], we made substantial upgrades to the powered hip exoskeleton hardware. First, we moved from a unilateral to a bilateral configuration in which assistance is provided to both hip joints. Then, we redesigned the pelvis interface and thigh cuff, moving from a soft textile-like structure to a semi-rigid interface sized to fit each user. Finally, we used more reliable cables and connectors to interface the main electronic board, located in the pelvis interface, with the actuators in the exoskeleton thigh segments. These design changes are described in our preliminary validation study with healthy individuals[37].

Each actuator features a five-bar linkage based on an offset slider crank and includes a high-efficiency ball screw (Fig. 4a). The hip exoskeleton has a peak torque of 45 Nm in flexion and extension. The pelvis interface integrates the electronics and battery into a rigid frame that connects to the user through BOA straps (BOA Technology Inc.) and flexible 3D printed orthoses. The thigh interface includes an anterior stiff 3D printed frame and a flexible wrap-around cuff with a posterior BOA closure. The passive degrees of freedom in the powered hip exoskeleton create a self-aligning mechanism similar to the system described in our previous work[95], which has been shown to improve users' comfort and performance[96]. The 3D printed interfaces can be adjusted to fit different users, and the BOA straps feature ratcheting dials to provide customizable tightening levels.

Assistive controller

As in our previous studies[37,62,63], the hip exoskeleton's embedded control system runs an assistive controller based on adaptive frequency oscillators[97–99] (Fig. 4b). The controller has a 0-100% gait cycle with a flexion torque gaussian profile and extension torque gaussian profile. The magnitude, width, and location of each gaussian in the gait cycle can be independently controlled for each side. These parameters were tuned for each participant before the start of the experiment. Tuning was completed independently for the participants' affected and unaffected hip joints. Tuning was based on feedback from the participants and the experimenter's judgment.

Data processing and statistical analyses

The modified Brockway equation was used to calculate body weight normalized metabolic power over the last two minutes of the standing and walking trials[64]. Net metabolic power was obtained by subtracting the average metabolic power measured during the standing baseline trial from the average metabolic power measured during each walking trial. The metabolic cost of transport was calculated for each walking trial by dividing the metabolic power of each participant by their walking speed[67].

The exoskeleton performance index quantifies the ratio between the change in metabolic power and average exoskeleton positive mechanical power provided, scaled by the muscular efficiency factor of 0.25[66]. We use this muscular efficiency factor based on work indicating that human muscles perform positive mechanical work with a muscular efficiency that asymptotically approaches 0.25[69].

We evaluated interlimb asymmetry during both walking trials using a symmetry index (SI). The SI is calculated by taking the difference between the spatiotemporal data of the affected and unaffected sides, divided by one-half the sum of the spatiotemporal data from both sides, multiplied by 100%[36]. A positive SI indicates asymmetry towards the subject's unaffected side, while a negative SI indicates asymmetry towards the subject's affected side. Zero indicates perfect symmetry.

Motion capture data were analyzed offline using Nexus 2.16 (Vicon Motion Systems, Ltd., Oxford, U.K.), Visual 3D (C-Motion, Maryland, USA), and MATLAB 2024b (MathWorks, Inc., Massachusetts, USA). Core processing in Nexus produced 3D trajectories and joint centers from the raw marker data and calibrated joint positions using SCoRE and SARA. The marker trajectories, force plate analog data, and exoskeleton data were imported into Visual 3D. Marker trajectories and force plate measurements were digitally lowpass filtered using bidirectional, fourth-order Butterworth filters at 6 Hz and 15 Hz, respectively. Kinematics and kinetics were computed using the V3D Composite Pelvis[100]. All inverse dynamic calculations were computed in Visual 3D and imported into MATLAB for subsequent analysis. Trajectories from the inverse dynamic calculations were digitally lowpass filtered using a bidirectional, second-order Butterworth filter at 6 Hz.

As is commonly done in the powered exoskeleton field[30,101,102], we calculated the biological torque produced by the participants by assuming that the exoskeleton perfectly transfers its desired assistance to the user. Thus, the biological hip torque was calculated by subtracting the assistive torque provided by the exoskeleton from the total hip torque calculated through inverse dynamics.

After stride-time normalization, we first calculated the average kinematic and kinetic profiles for each subject across strides, and then the average across the resultant subject means. We also calculated the average maximum values for each subject across strides, and then the average across the resultant subject means. Interparticipant means and standard errors are reported unless otherwise indicated.

Joint work was calculated as the time integral of power during each stride. Energetic analyses of the affected and unaffected hip joints were further divided into the subphases of a stride. Specifically, these phases are identified as initial double support, single support, terminal double support, and swing. Initial double support lasts from the ipsilateral heel strike to the contralateral toe-off, then single support occurs until the contralateral heel strike. Terminal double support occurs until the ipsilateral toe-off, and finally, swing occurs from the ipsilateral toe-off to heel strike.

Two-tailed paired t-tests evaluated effects of exoskeleton assistance on our primary outcome measures: metabolic power, total positive biological work (affected and unaffected hip, knee, and ankle joints, summed), and positive biological hip work (affected and unaffected hip joints, summed). We set $\alpha = 0.05$ for these analyses and applied a

Holm-Bonferroni correction to adjust for multiple comparisons. We did not statistically compare any secondary outcome measures (hip work during stance, foot clearance, kinematics, kinetics). We used a two-tailed t-test because we did not have a prior assumption that the difference between conditions (walking with or without the exoskeleton) would be positive or negative. Finally, the data were normally distributed and there were no outliers, meeting the requirements for a two-tailed paired t-test.

To evaluate changes in kinematic trajectories during walking with the exoskeleton compared to walking without the exoskeleton, we performed a 1-dimensional Statistical Parametric Map (SPM) analysis, using the spm1d 0.4.10 package in Matlab 2024b[103]. SPM was run on the kinematic trajectories of each joint (affected and unaffected hip, knee, and ankle) during walking with the exoskeleton compared to walking without the exoskeleton to identify statistically significant changes (two-tailed paired t-tests with $\alpha = 0.05$).

Data Availability

All data supporting the findings of this study are available within the article and its supplementary files. Any additional requests for information can be directed to, and will be fulfilled by, the corresponding author. Source data are provided with this paper. All data generated in this study have been deposited in a *figshare* repository [https://doi.org/10.6084/m9.figshare.30158260].

Code Availability

This work does not use any custom computer code or software.

References

1. Michael, K. M., Allen, J. K. & Macko, R. F. Reduced Ambulatory Activity After Stroke: The Role of Balance, Gait, and Cardiovascular Fitness. *Arch Phys Med Rehabil* **86**, 1552–1556 (2005).
2. Clarke, P. & Black, S. E. Quality of Life Following Stroke: Negotiating Disability, Identity, and Resources. *Journal of Applied Gerontology* **24**, 319–336 (2005).
3. Lloyd-Jones, D. *et al.* Heart Disease and Stroke Statistics—2010 Update. *Circulation* **121**, (2010).
4. Cruz, T. H., Lewek, M. D. & Dhaher, Y. Y. Biomechanical impairments and gait adaptations post-stroke: Multi-factorial associations. *J Biomech* **42**, 1673–1677 (2009).
5. Moriello, C., Finch, L. & Mayo, N. E. Relationship between muscle strength and functional walking capacity among people with stroke. *The Journal of Rehabilitation Research and Development* **48**, 267 (2011).
6. Thibaut, A. *et al.* Spasticity after stroke: Physiology, assessment and treatment. *Brain Inj* **27**, 1093–1105 (2013).
7. Lord, S. E., McPherson, K., McNaughton, H. K., Rochester, L. & Weatherall, M. Community ambulation after stroke: how important and obtainable is it and what measures appear predictive? *Arch Phys Med Rehabil* **85**, 234–239 (2004).
8. Franceschini, M. *et al.* Walking Performance: Correlation between Energy Cost of Walking and Walking Participation. New Statistical Approach Concerning Outcome Measurement. *PLoS One* **8**, e56669 (2013).
9. English, C., Manns, P. J., Tucak, C. & Bernhardt, J. Physical Activity and Sedentary Behaviors in People With Stroke Living in the Community: A Systematic Review. *Phys Ther* **94**, 185–196 (2014).
10. Olney, S. J. & Richards, C. Hemiparetic gait following stroke. Part I: Characteristics. *Gait Posture* **4**, 136–148 (1996).
11. Combs, S. A. *et al.* Is walking faster or walking farther more important to persons with chronic stroke? *Disabil Rehabil* **35**, 860–867 (2013).
12. Xu, T. *et al.* Risk Factors for Falls in Community Stroke Survivors: A Systematic Review and Meta-Analysis. *Arch Phys Med Rehabil* **99**, 563-573.e5 (2018).
13. Brouwer, B., Parvataneni, K. & Olney, S. J. A comparison of gait biomechanics and metabolic requirements of overground and treadmill walking in people with stroke. *Clinical Biomechanics* **24**, 729–734 (2009).
14. Li, S., Francisco, G. E. & Zhou, P. Post-stroke Hemiplegic Gait: New Perspective and Insights. *Front Physiol* **9**, (2018).
15. Nagano, H., Said, C. M., James, L., Sparrow, W. A. & Begg, R. Biomechanical Correlates of Falls Risk in Gait Impaired Stroke Survivors. *Front Physiol* **13**, (2022).
16. Geerars, M., Minnaar-van der Feen, N. & Huisstede, B. M. A. Treatment of knee hyperextension in post-stroke gait. A systematic review. *Gait Posture* **91**, 137–148 (2022).
17. Appasamy, M. *et al.* Treatment Strategies for Genu Recurvatum in Adult Patients With Hemiparesis: A Case Series. *PM&R* **7**, 105–112 (2015).
18. Hada, S. *et al.* The degeneration and destruction of femoral articular cartilage shows a greater degree of deterioration than that of the tibial and patellar articular cartilage in early stage knee osteoarthritis: a cross-sectional study. *Osteoarthritis Cartilage* **22**, 1583–1589 (2014).
19. Darak, V. & Karthikbabu, S. Lower limb motor function and hip muscle weakness in stroke survivors and their relationship with pelvic tilt, weight-bearing asymmetry, and gait speed: A cross-sectional study. *Curr J Neurol* **26**, 2097–101; discussion 2102 (2020).
20. Rybar, M. M. *et al.* The stroke-related effects of hip flexion fatigue on over ground walking. *Gait Posture* **39**, 1103–1108 (2014).
21. Chen, G., Patten, C., Kothari, D. H. & Zajac, F. E. Gait differences between individuals with post-stroke hemiparesis and non-disabled controls at matched speeds. *Gait Posture* **22**, 51–56 (2005).
22. Ganley, K. J., Herman, R. M. & Willis, W. T. Muscle Metabolism During Overground Walking in Persons with Poststroke Hemiparesis. *Top Stroke Rehabil* **15**, 218–226 (2008).
23. Farris, D. J., Hampton, A., Lewek, M. D. & Sawicki, G. S. Revisiting the mechanics and energetics of walking in individuals with chronic hemiparesis following stroke: from individual limbs to lower limb joints. *J Neuroeng Rehabil* **12**, 24 (2015).
24. Platts, M. M., Rafferty, D. & Paul, L. Metabolic Cost of Overground Gait in Younger Stroke Patients and Healthy Controls. *Med Sci Sports Exerc* **38**, 1041–1046 (2006).
25. Siviy, C. *et al.* Opportunities and challenges in the development of exoskeletons for locomotor assistance. *Nat Biomed Eng* **7**, 456–472 (2022).
26. de Miguel-Fernandez, J. *et al.* Immediate Biomechanical Effects of Providing Adaptive Assistance With an Ankle Exoskeleton in Individuals After Stroke. *IEEE Robot Autom Lett* **7**, 7574–7580 (2022).
27. Awad, L. N. *et al.* A soft robotic exosuit improves walking in patients after stroke. *Sci Transl Med* **9**, (2017).
28. Takahashi, K. Z., Lewek, M. D. & Sawicki, G. S. A neuromechanics-based powered ankle exoskeleton to assist walking post-stroke: a feasibility study. *J Neuroeng Rehabil* **12**, 23 (2015).
29. Swaminathan, K. *et al.* Ankle-targeted exosuit resistance increases paretic propulsion in people post-stroke. *J Neuroeng Rehabil* **20**, 85 (2023).
30. McCain, E. M. *et al.* Mechanics and energetics of post-stroke walking aided by a powered ankle exoskeleton with speed-adaptive myoelectric control. *J Neuroeng Rehabil* **16**, 57 (2019).
31. Sloutsky, R. *et al.* Targeting post-stroke walking automaticity with a propulsion-augmenting soft robotic exosuit: toward a biomechanical and neurophysiological approach to assistance prescription. in *2021 10th International IEEE/EMBS Conference on Neural Engineering (NER)* vols 2021-May 862–865 (IEEE, Italy, 2021).
32. Browning, R. C., Modica, J. R., Kram, R. & Goswami, A. The Effects of Adding Mass to the Legs on the Energetics and Biomechanics of Walking. *Med Sci Sports Exerc* **39**, 515–525 (2007).
33. Bae, J. *et al.* A Lightweight and Efficient Portable Soft Exosuit for Paretic Ankle Assistance in Walking After Stroke. in *2018 IEEE International Conference on Robotics and Automation (ICRA)* 2820–2827 (IEEE, Brisbane, QLD, Australia, 2018). doi:10.1109/ICRA.2018.8461046.
34. Awad, L. N., Kudzia, P., Revi, D. A., Ellis, T. D. & Walsh, C. J. Walking Faster and Farther With a Soft Robotic Exosuit: Implications for Post-Stroke Gait Assistance and Rehabilitation. *IEEE Open J Eng Med Biol* **1**, 108–115 (2020).
35. Sloot, L. H. *et al.* Effects of a soft robotic exosuit on the quality and speed of overground walking depends on walking ability after stroke. *J Neuroeng Rehabil* **20**, 113 (2023).
36. Bae, J. *et al.* Biomechanical mechanisms underlying exosuit-induced improvements in walking economy after stroke. *Journal of Experimental Biology* https://doi.org/10.1242/jeb.168815 (2018) doi:10.1242/jeb.168815.
37. Ishmael, M. K., Archangeli, D. & Lenzi, T. A Powered Hip Exoskeleton With High Torque Density for Walking, Running, and Stair Ascent. *IEEE/ASME Transactions on Mechatronics* **27**, 4561–4572 (2022).
38. Zhang, X. *et al.* A Lower Limb Wearable Exosuit for Improved Sitting, Standing, and Walking Efficiency. *IEEE Transactions on Robotics* **41**, 127–140 (2025).
39. Seo, K., Lee, J. & Park, Y. J. Autonomous hip exoskeleton saves metabolic cost of walking uphill. in *2017 International Conference on Rehabilitation Robotics (ICORR)* 246–251 (IEEE, London, UK, 2017). doi:10.1109/ICORR.2017.8009254.
40. Seo, K., Lee, J., Lee, Y., Ha, T. & Shim, Y. Fully autonomous hip exoskeleton saves metabolic cost of walking. in *2016 IEEE International Conference on Robotics and Automation (ICRA)* 4628–4635 (IEEE, Stockholm, Sweden, 2016). doi:10.1109/ICRA.2016.7487663.
41. Winter, D. Human balance and posture control during standing and walking. *Gait Posture* **3**, 193–214 (1995).
42. Roche, N., Bonnyaud, C., Geiger, M., Bussel, B. & Bensmail, D. Relationship between hip flexion and ankle dorsiflexion during swing

phase in chronic stroke patients. *Clinical Biomechanics* **30**, 219–225 (2015).
43. Mueller, M. J., Minor, S. D., Sahrmann, S. A., Schaaf, J. A. & Strube, M. J. Differences in the Gait Characteristics of Patients With Diabetes and Peripheral Neuropathy Compared With Age-Matched Controls. *Phys Ther* **74**, 299–308 (1994).
44. Mueller, M. J., Sinacore, D. R., Hoogstrate, S. & Daly, L. Hip and ankle walking strategies: Effect on peak plantar pressures and implications for neuropathic ulceration. *Arch Phys Med Rehabil* **75**, 1196–1200 (1994).
45. Fallah, N. & Beck, O. N. The metabolic cost of producing joint moments is greater at the hip than at the ankle. *Journal of Experimental Biology* **228**, (2025).
46. Molinaro, D. D., Kang, I. & Young, A. J. Estimating human joint moments unifies exoskeleton control, reducing user effort. *Sci Robot* **9**, (2024).
47. Young, A. J., Foss, J., Gannon, H. & Ferris, D. P. Influence of Power Delivery Timing on the Energetics and Biomechanics of Humans Wearing a Hip Exoskeleton. *Front Bioeng Biotechnol* **5**, (2017).
48. Lim, B. *et al.* Delayed Output Feedback Control for Gait Assistance With a Robotic Hip Exoskeleton. *IEEE Transactions on Robotics* **35**, 1055–1062 (2019).
49. Lee, J. *et al.* Effects of assistance timing on metabolic cost, assistance power, and gait parameters for a hip-type exoskeleton. in *2017 International Conference on Rehabilitation Robotics (ICORR)* 498–504 (IEEE, London, UK, 2017). doi:10.1109/ICORR.2017.8009297.
50. Manzoori, A. R. *et al.* Adaptive hip exoskeleton control using heart rate feedback reduces oxygen cost during ecological locomotion. *Sci Rep* **15**, 507 (2025).
51. Kim, J. *et al.* Reducing the metabolic rate of walking and running with a versatile, portable exosuit. *Science (1979)* **365**, 668–672 (2019).
52. Lee, H.-J. *et al.* A Wearable Hip Assist Robot Can Improve Gait Function and Cardiopulmonary Metabolic Efficiency in Elderly Adults. *IEEE Transactions on Neural Systems and Rehabilitation Engineering* **25**, 1–1 (2017).
53. Lee, Y. *et al.* A flexible exoskeleton for hip assistance. in *2017 IEEE/RSJ International Conference on Intelligent Robots and Systems (IROS)* 1058–1063 (IEEE, Vancouver, BC, Canada, 2017). doi:10.1109/IROS.2017.8202275.
54. Cao, W., Chen, C., Hu, H., Fang, K. & Wu, X. Effect of Hip Assistance Modes on Metabolic Cost of Walking With a Soft Exoskeleton. *IEEE Transactions on Automation Science and Engineering* **18**, 426–436 (2021).
55. Kim, J. *et al.* Reducing the energy cost of walking with low assistance levels through optimized hip flexion assistance from a soft exosuit. *Sci Rep* **12**, 11004 (2022).
56. Luo, S. *et al.* Experiment-free exoskeleton assistance via learning in simulation. *Nature* **630**, 353–359 (2024).
57. Archangeli, D., Ishmael, M. K. & Lenzi, T. Assistive Powered Hip Exoskeleton Improves Self-Selected Walking Speed in One Individual with Hemiparesis: A Case Study. in *2022 International Conference on Rehabilitation Robotics (ICORR)* vols 2022-July 1–6 (IEEE, Rotterdam, Netherlands, 2022).
58. Pan, Y.-T. *et al.* Effects of Bilateral Assistance for Hemiparetic Gait Post-Stroke Using a Powered Hip Exoskeleton. *Ann Biomed Eng* **51**, 410–421 (2023).
59. Livolsi, C. *et al.* Bilateral hip exoskeleton assistance enables faster walking in individuals with chronic stroke-related gait impairments. *Sci Rep* **15**, 2017 (2025).
60. Herrin, K., Upton, E. & Young, A. Towards meaningful community ambulation in individuals post stroke through use of a smart hip exoskeleton: A preliminary investigation. *Assistive Technology* **36**, 198–208 (2024).
61. Nuckols, R. W. *et al.* Mobile Unilateral Hip Flexion Exosuit Assistance for Overground Walking in Individuals Post-Stroke: A Case Series. in *Proceedings of the 5th International Symposium on Wearable Robotics, WeRob2020, and of WearRAcon Europe 2020, October 13–16, 2020* 357–361 (2022). doi:10.1007/978-3-030-69547-7_58.
62. Ishmael, M. K. *et al.* Powered Hip Exoskeleton Reduces Residual Hip Effort Without Affecting Kinematics and Balance in Individuals With Above-Knee Amputations During Walking. *IEEE Trans Biomed Eng* **70**, 1162–1171 (2023).
63. Ishmael, M. K., Archangeli, D. & Lenzi, T. Powered hip exoskeleton improves walking economy in individuals with above-knee amputation. *Nat Med* **27**, 1783–1788 (2021).
64. Brockway, J. M. Derivation of formulae used to calculate energy expenditure in man. *Hum Nutr Clin Nutr* **41**, 463–71 (1987).
65. Mooney, L. M., Rouse, E. J. & Herr, H. M. Autonomous exoskeleton reduces metabolic cost of human walking during load carriage. *J Neuroeng Rehabil* **11**, 80 (2014).
66. Sawicki, G. S. & Ferris, D. P. Mechanics and energetics of level walking with powered ankle exoskeletons. *Journal of Experimental Biology* **211**, 1402–1413 (2008).
67. Zarrugh, M. Y., Todd, F. N. & Ralston, H. J. Optimization of energy expenditure during level walking. *Eur J Appl Physiol Occup Physiol* **33**, 293–306 (1974).
68. Quinlivan, B. T. *et al.* Assistance magnitude versus metabolic cost reductions for a tethered multiarticular soft exosuit. *Sci Robot* **2**, 4416 (2017).
69. Margaria, R. Positive and negative work performances and their efficiencies in human locomotion. *Int Z Angew Physiol Einschl Arbeitsphysiol* **25**, 339–351 (1968).
70. Galle, S., Malcolm, P., Collins, S. H. & De Clercq, D. Reducing the metabolic cost of walking with an ankle exoskeleton: interaction between actuation timing and power. *J Neuroeng Rehabil* **14**, 35 (2017).
71. Esquenazi, A., Ofluoglu, D., Hirai, B. & Kim, S. The Effect of an Ankle-Foot Orthosis on Temporal Spatial Parameters and Asymmetry of Gait in Hemiparetic Patients. *PM&R* **1**, 1014–1018 (2009).
72. Pongpipatpaiboon, K. *et al.* The impact of ankle-foot orthoses on toe clearance strategy in hemiparetic gait: A cross-sectional study. *J Neuroeng Rehabil* **15**, (2018).
73. Pruyn, K., Murray, R., Gabert, L. & Lenzi, T. Autonomous Powered Ankle Exoskeleton Improves Foot Clearance and Knee Hyperextension After Stroke: A Case Study. *IEEE Trans Med Robot Bionics* **7**, 51–58 (2025).
74. van Swigchem, R., Roerdink, M., Weerdesteyn, V., Geurts, A. C. & Daffertshofer, A. The Capacity to Restore Steady Gait After a Step Modification Is Reduced in People With Poststroke Foot Drop Using an Ankle-Foot Orthosis. *Phys Ther* **94**, 654–663 (2014).
75. Vistamehr, A., Kautz, S. A. & Neptune, R. R. The influence of solid ankle-foot-orthoses on forward propulsion and dynamic balance in healthy adults during walking. *Clinical Biomechanics* **29**, 583–589 (2014).
76. Moore, J. L., Roth, E. J., Killian, C. & Hornby, T. G. Locomotor Training Improves Daily Stepping Activity and Gait Efficiency in Individuals Poststroke Who Have Reached a "Plateau" in Recovery. *Stroke* **41**, 129–135 (2010).
77. Lohse, K. R., Lang, C. E. & Boyd, L. A. Is More Better? Using Metadata to Explore Dose–Response Relationships in Stroke Rehabilitation. *Stroke* **45**, 2053–2058 (2014).
78. Hornby, T. G. *et al.* Variable Intensive Early Walking Poststroke (VIEWS). *Neurorehabil Neural Repair* **30**, 440–450 (2016).
79. Schmid, A. A. *et al.* Balance and Balance Self-Efficacy Are Associated With Activity and Participation After Stroke: A Cross-Sectional Study in People With Chronic Stroke. *Arch Phys Med Rehabil* **93**, 1101–1107 (2012).
80. Norlander, A. *et al.* Long-Term Predictors of Social and Leisure Activity 10 Years after Stroke. *PLoS One* **11**, e0149395 (2016).
81. Kleim, J. A. & Jones, T. A. Principles of Experience-Dependent Neural Plasticity: Implications for Rehabilitation After Brain Damage. *J Speech Lang Hear Res* **51**, (2008).
82. Sheffler, L. R. & Chae, J. Technological Advances in Interventions to Enhance Poststroke Gait. *Phys Med Rehabil Clin N Am* **24**, 305–323 (2013).
83. Zhang, J. *et al.* Human-in-the-loop optimization of exoskeleton assistance during walking. *Science (1979)* **356**, 1280–1284 (2017).

84. Durandau, G., Rampeltshammer, W. F., Kooij, H. van der & Sartori, M. Neuromechanical Model-Based Adaptive Control of Bilateral Ankle Exoskeletons: Biological Joint Torque and Electromyogram Reduction Across Walking Conditions. *IEEE TRO* **38**, 1380–1394 (2022).
85. Stensgaard Stoltze, J., Rasmussen, J. & Skipper Andersen, M. On the biomechanical relationship between applied hip, knee and ankle joint moments and the internal knee compressive forces. *Int Biomech* **5**, 63–74 (2018).
86. Poggensee, K. L. & Collins, S. H. How adaptation, training, and customization contribute to benefits from exoskeleton assistance. *Sci Robot* **6**, 185–196 (2021).
87. Lakmazaheri, A. *et al.* Optimizing exoskeleton assistance to improve walking speed and energy economy for older adults. *J Neuroeng Rehabil* **21**, (2024).
88. Galle, S., Malcolm, P., Derave, W. & De Clercq, D. Adaptation to walking with an exoskeleton that assists ankle extension. *Gait Posture* **38**, 495–499 (2013).
89. Ferrarello, F. *et al.* Tools for Observational Gait Analysis in Patients With Stroke: A Systematic Review. *Phys Ther* **93**, 1673–1685 (2013).
90. Guidetti, L. *et al.* Validity, reliability and minimum detectable change of COSMED K5 portable gas exchange system in breath-by-breath mode. *PLoS One* **13**, e0209925 (2018).
91. Reinkensmeyer, D., Wynne, J. H. & Harkema, S. J. A robotic tool for studying locomotor adaptation and rehabilitation. in *Proceedings of the Second Joint 24th Annual Conference and the Annual Fall Meeting of the Biomedical Engineering Society Engineering in Medicine and Biology* 2353–2354 (IEEE, Houston, TX, 2002). doi:10.1109/IEMBS.2002.1053318.
92. Hood, S., Ishmael, M. K., Gunnell, A., Foreman, K. B. & Lenzi, T. A kinematic and kinetic dataset of 18 above-knee amputees walking at various speeds. *Sci Data* **7**, (2020).
93. Ehrig, R. M., Taylor, W. R., Duda, G. N. & Heller, M. O. A survey of formal methods for determining the centre of rotation of ball joints. *J Biomech* **39**, 2798–2809 (2006).
94. Stagni, R., Fantozzi, S. & Cappello, A. Double calibration versus global otpimisation: Performance and effectiveness for clinical application. *Gait Posture* **24**, S17–S18 (2006).
95. Sarkisian, S. V., Ishmael, M. K., Hunt, G. R. & Lenzi, T. Design, Development, and Validation of a Self-Aligning Mechanism for High-Torque Powered Knee Exoskeletons. *IEEE Trans Med Robot Bionics* **2**, 248–259 (2020).
96. Sarkisian, S. V., Ishmael, M. K. & Lenzi, T. Self-Aligning Mechanism Improves Comfort and Performance With a Powered Knee Exoskeleton. *IEEE TNSRE* **29**, 629–640 (2021).
97. Ronsse, R. *et al.* Human–Robot Synchrony: Flexible Assistance Using Adaptive Oscillators. *IEEE Trans Biomed Eng* **58**, 1001–1012 (2011).
98. Lenzi, T., Carrozza, M. C. & Agrawal, S. K. Powered Hip Exoskeletons Can Reduce the User's Hip and Ankle Muscle Activations During Walking. *IEEE TNSRE* **21**, 938–948 (2013).
99. Ronsse, R. *et al.* Oscillator-based assistance of cyclical movements: model-based and model-free approaches. *Med Biol Eng Comput* **49**, 1173–1185 (2011).
100. C-Motion WIKI Documentation. V3D Composite Pelvis. (2019).
101. Collins, S. H., Wiggin, M. B. & Sawicki, G. S. Reducing the energy cost of human walking using an unpowered exoskeleton. *Nature* **522**, 212–215 (2015).
102. Farris, D. J. & Sawicki, G. S. Linking the mechanics and energetics of hopping with elastic ankle exoskeletons. *J Appl Physiol* **113**, 1862–1872 (2012).
103. Pataky, T. SPM1D spatial parametric map. Preprint at https://spm1d.org/index (2022).

Acknowledgments

We wish to acknowledge the contribution of all study participants. We thank S. Edgely for helping with participant recruitment.

This study was funded in part by National Institute for Occupational Safety and Health under grant number T42OH008414 (T.L., K.P.), in part by the National Science Foundation under grant number 2046287 (T.L.), in part by National Science Foundation Graduate Research Fellowship Program under grant number 2139322 (K.P.), and in part by the National Institutes of Health under project 1T32TR004394-0 (R.M.).

Author Contributions

T.L. supervised all aspects of the project. K.P., R.M., L.G., and T.L. developed the exoskeleton and controller. K.P., R.M., and T.L. conducted human experiments. K.P., R.M., L.G., B.F., and T.L. analyzed the data. All authors contributed to manuscript preparation.

Competing Interests Statement

The authors declare no competing interests.

Correspondence and requests for materials should be addressed to Tommaso Lenzi.

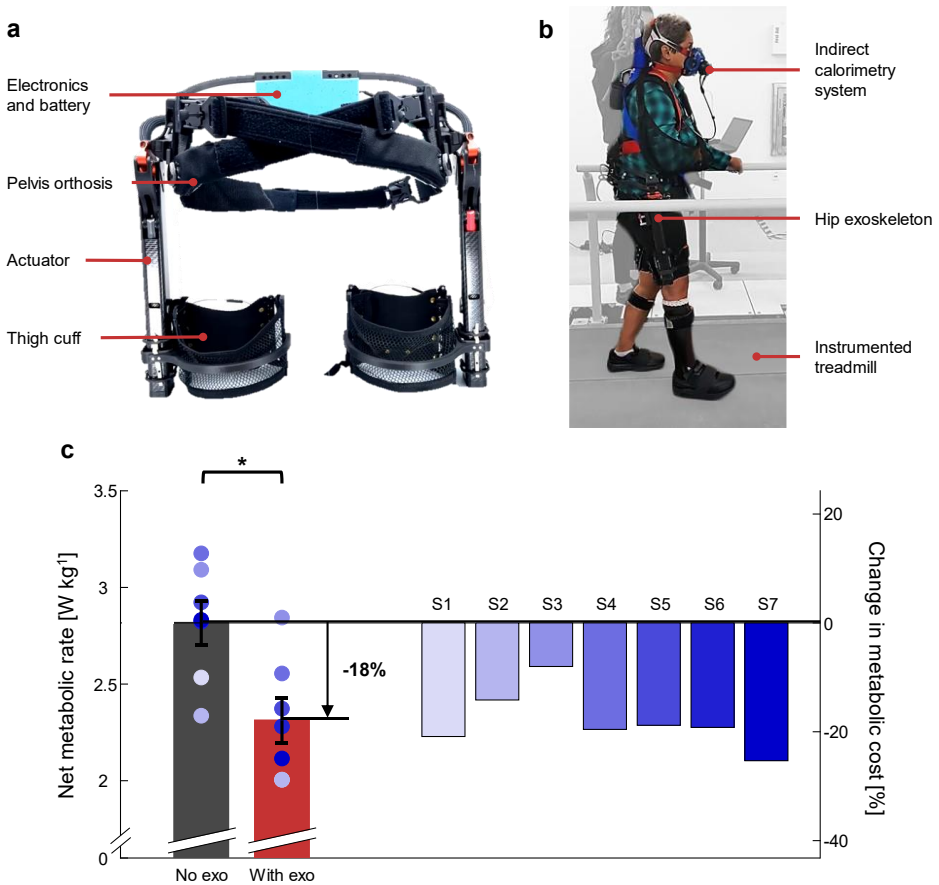

Fig. 1 | Metabolic cost of walking. (**a**) The powered hip exoskeleton used in this study. (**b**) Subject walking with the hip exoskeleton during the metabolic cost evaluation. (**c**) Body weight normalized net metabolic rate during walking, averaged across all participants without the exoskeleton (gray) and with the exoskeleton (red). The square bracket shows the result of the two-tailed paired t-test (P = 0.0002, n = 7). Individual participant metabolic rates are shown with the blue dots, corresponding to the bars representing their individual percent change in metabolic cost. The bars represent the mean, and the error bars represent the standard error. Figure (**c**) generated in MATLAB 2024b (MathWorks, Inc., Massachusetts, USA).

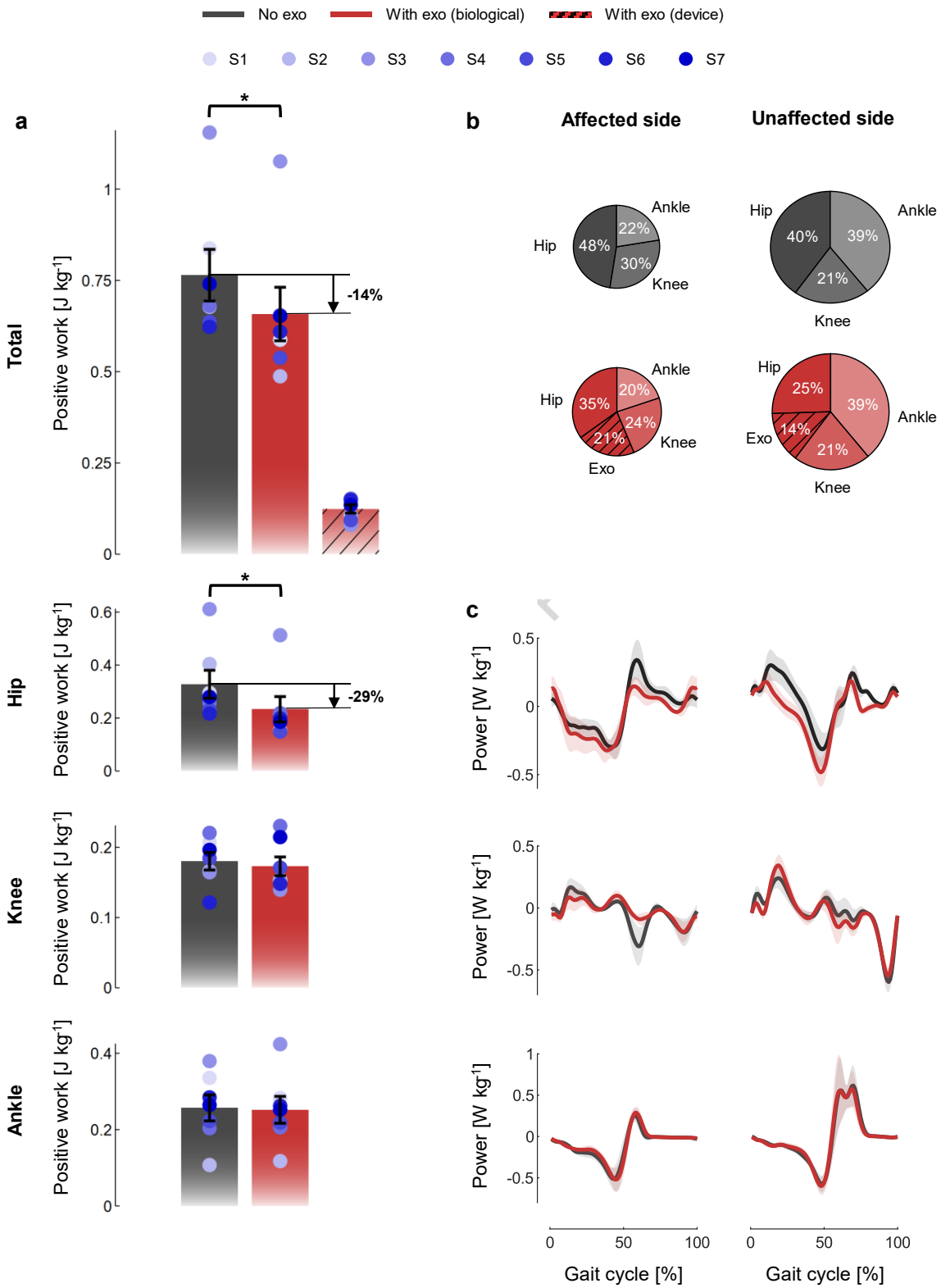

Fig. 2| Joint work and power. All data are body weight normalized, where the gray represents the biological values without the exoskeleton, and the red represents the biological values with the exoskeleton. A cross-hatched red represents the exoskeleton contributions with the exoskeleton. The blue dots (**a**) represent values for the individual participants. The bars (**a**) and the solid lines (**c**) represent the mean, and the error bars (**a**) and shaded regions (**c**) represent the standard error. Brackets indicate that statistical tests were performed to compare the two conditions, and asterisks indicate significant differences. (**a**) The total positive biological work done by the lower limb joints (affected and unaffected hips, knees, and ankles, summed) and the positive work generated by the exoskeleton (affected and unaffected hips, summed). The square bracket shows the result of the two-tailed paired t-test ($P = 0.0167$, $n = 7$). The positive biological work generated by both the affected and unaffected hip (top), knee (middle), and ankle (bottom) joints. The square bracket shows the result of the two-tailed paired t-test for positive biological hip work ($P = 0.0052$, $n = 7$). (**b**) Pie charts representing the average percent contributions of each lower limb joint and the exoskeleton to the positive work done by each side. Each chart is scaled based on the total positive work done by the unaffected side without the exoskeleton. The left column represents the affected side, and the right column represents the unaffected side. (**c**) The power trajectories for all lower limb joints over the gait cycle, where the left column represents the affected joints, and the right column represents the unaffected joints. Figure generated in MATLAB 2024b (MathWorks, Inc., Massachusetts, USA).

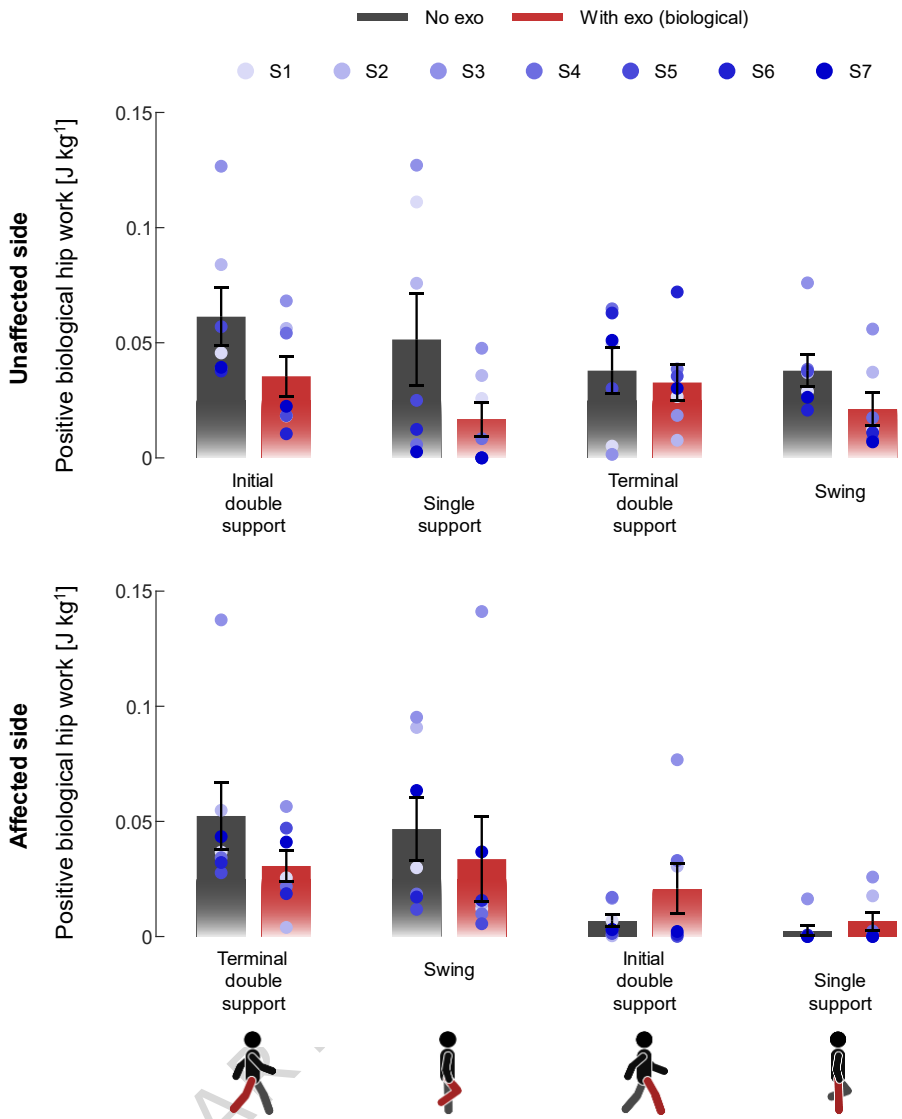

Fig. 3 | Positive biological hip work during the phases of stance and swing. Body weight normalized positive biological hip work during each phase of stance (initial double support, single support, terminal double support) and swing without the exoskeleton (gray) and with the exoskeleton (red). The phases of the affected side (top) are time-aligned with the phases of the unaffected side (bottom), as shown in the walking diagram, where red is the affected leg and gray is the unaffected leg. The bars represent the mean, and the error bars represent the standard error. The positive biological hip work done by individual participants on each side during each phase is shown with the blue dots. Figure generated in MATLAB 2024b (MathWorks, Inc., Massachusetts, USA).

Table 1. Participant baseline characteristics.

Participant	Paretic side	Sex	Age (years)	Chronicity (years)	Orthosis	Walking speed (m s^{-1})	Height (m)	Weight (kg)	Avg handrail force (% BW) no exo / exo
1	Left	Female	58	13	None	0.58	1.7	70	3.8 / 3.7
2	Right	Female	50	3	AFO	0.37	1.6	77	4.6 / 5.4
3	Right	Male	34	8	None	1.00	1.8	73	0.1 / 0.4
4	Right	Male	30	9	None	0.85	1.6	74	3.4 / 3.9
5	Right	Male	36	8	None	0.60	1.7	102	0.3 / 0.1
6	Left	Male	46	4	AFO	0.50	1.8	82	5.1 / 4.6
7	Right	Male	29	5	None	0.90	1.8	87	1.6 / 1.5

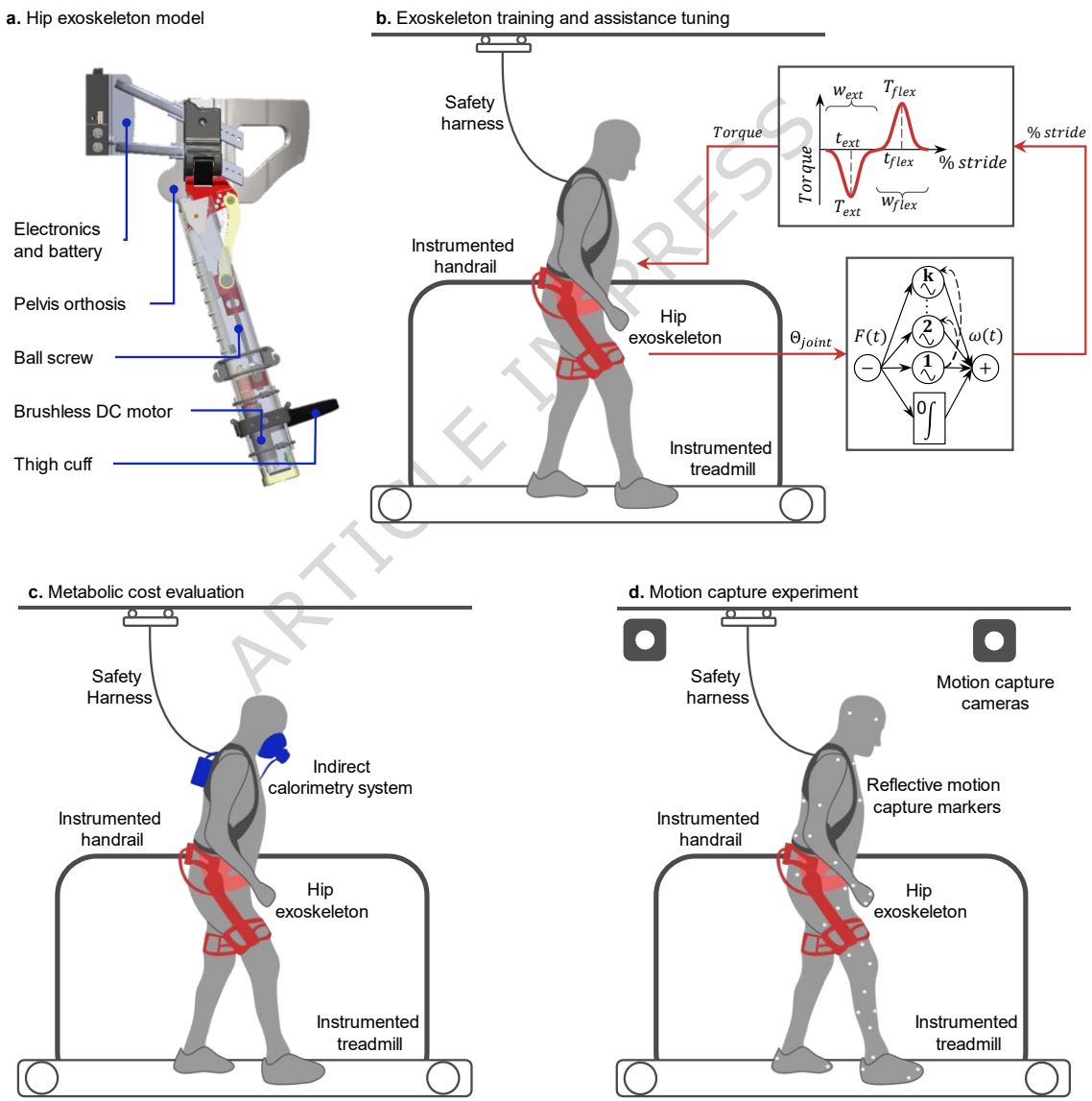

Fig. 4 | Experimental Methods. Participants came in approximately once a week until they completed the training and testing sessions. (**a**) A model of the powered hip exoskeleton with transparency to show the actuation system. The exoskeleton comprises a three-dimensional (3D) printed orthosis strapped to the pelvis and a cuff that wraps around the user's thigh. The actuation system includes a brushless DC motor, helical gears, a ball screw, and a composite spring. A passive abduction/adduction joint acts in series to the powered flexion/extension joint. (**b**) The study participants completed a series of exoskeleton training sessions in which they adapted to walking with exoskeleton assistance, and the experimenter manually tuned the flexion/extension assistance for each leg. The exoskeleton's embedded control system runs an assistive controller based on adaptive frequency oscillators[97–99]. (**c**) After completing the training and tuning sessions, we measured the metabolic cost of walking with and without the exoskeleton. (**d**) The final testing session took place in a motion capture lab, where participants completed the same series of walking trials that they completed with and without the exoskeleton during the metabolic cost evaluation.

Editorial Summary

Stroke often leads to walking impairment. Here, the authors show that assistance from a lightweight, portable, bilateral hip exoskeleton reduces the metabolic cost of walking by 18% for individuals with post-stroke hemiparesis.

Peer review information: *Nature Communications* thanks Chenglong Fu and the other, anonymous, reviewer(s) for their contribution to the peer review of this work. A peer review file is available.